International Journal of Engineering Research and Technology. ISSN 0974-3154, Volume 12, Number 11 (2019), pp. 2023-2030

Output-Only Damage Detection Using Neural Network and Sensor Clustering Under Ambient Vibration

Sarehati Umar[1], Mohammadreza Vafaei[2], Sophia C. Alih[1,3]

[1]*School of Civil Engineering, Faculty of Engineering, Universiti Teknologi Malaysia, 81310 Johor Bahru, Malaysia.*

[2]*Forensic Engineering Center, School of Civil Engineering, Faculty of Engineering, Universiti Teknologi Malaysia, 81310 Johor Bahru, Malaysia.*

[3]*Institute of Noise and Vibration, Universiti Teknologi Malaysia Kuala Lumpur (UTM KL), Jalan Sultan Yahya Petra, 54100 Kuala Lumpur, Malaysia.*

ORCIDs: 0000-0003-4871-7898 (Sarehati), 0000-0002-9988-1842(Mohammadreza), 0000-0001-5326-3670(Sophia C.)

Abstract

Time-series methods have become of interest in damage detection, particularly for automated and continuous structural health monitoring due to having no requirement for modal analysis or details of physical structural properties. Despite the success of the sensor clustering concept in improving the ability of time-series methods to detect, locate and quantify structural damage, most of the applications rely on free vibration response that can be obtained directly by impact testing, which is difficult to obtain for in-service structures, or indirectly by transforming the ambient vibration response. Therefore, the present study extends the use of sensor clustering for damage detection under ambient vibration by directly using the measured response. In this study, nonlinear autoregressive with exogenous inputs (NARX) system was modelled using artificial neural network for different sensor clusters using the acceleration response of the structure. The differences of the NARX neural network prediction errors are used as damage sensitive features to infer damage existence, location and severity. The applicability of the method is demonstrated using a numerical model of a two-span concrete slab under varying excitation conditions to simulate ambient vibration. The method performed successfully for single and multiple damage cases.

Keywords: Ambient vibration, Artificial neural network, Vibration-based damage detection, Sensor clustering, Time-series response

I. INTRODUCTION

Civil engineering infrastructures are subjected to deterioration owing to long term fatigue, environmental factors and severe loading events such as earthquakes. Early detection of structural damage is necessary for preventing catastrophic failure that leads to fatal consequences and tremendous economic losses. In this regard, structural health monitoring (SHM) has been intensively developed and progressed during the last few decades, particularly in using vibrational parameters to detect, locate, and quantify damage in a structure.

Vibration-based damage detection can be classified into frequency domain and time domain approaches. In frequency domain methods, damage can be detected by examining the feature changes extracted from frequency response functions (FRF) [1,2] or modal data (i.e., natural frequencies, mode shapes and derivatives) [3–5]. On the other hand, damage sensitive features (DSFs) in time domain methods are derived directly from the measured time-history responses (i.e., displacement, velocity and acceleration) [6,7].

Among time-domain methods, time-series analysis has gained attention recently due to high potential in automated SHM as it can directly process the large amount of continuous data acquired from multiple sensors. It is based on a methodology that aims to fit the measured responses into time-series models (i.e., autoregressive (AR) model, autoregressive with exogenous inputs (ARX) model, autoregressive moving average (ARMA) model, autoregressive moving average with exogenous input (ARMAX) model) and then damage detection is attempted using the extracted DSF formulated based on model coefficients [8–10] or residual errors [11–13]. Although the applications of time-series based techniques have shown great success at Level 1 damage identification [14], most of them are unable to provide further information about the damage, such as location (Level 2) and severity (Level 3).

Therefore, Gul and Catbas [15] introduced the sensor clustering concept to time-series analysis methodology to extend its applicability up to Level 3 damage identification. In their study, two DSFs based on the ARX model coefficient and fit ratio were extracted from data obtained from an impact test. Farahani and Penumadu [16] also applied the concept to a full-scale five-girder bridge using a drop-source test. To allow the sensor clustering applicable to ambient vibration, Gul and Catbas [17] improved the method by incorporating a random decrement (RD) to obtain pseudo-free response data while Mei and Gül [18] directly applied sensor clustering on ambient vibration data and used ARMAX model coefficients to identify damage.

In the above-mentioned studies, the methods are based on linear time-series models with free vibration response. Despite their good damage detection results, free response data is difficult to collect as impact vibration testing requires suspension of normal structure operation. Therefore, the present study made good use of artificial neural network (ANN) ability in learning linear and nonlinear systems to model nonlinear ARX (NARX) in conjunction with sensor clustering using output-only data, which is the acceleration response. The numerical structure of a two-span concrete slab was used to demonstrate the applicability of the proposed method under ambient vibration. To simulate a better representation of the actual ambient vibration tests, the amplitude, frequency and location of load excitation were randomised during the sampling duration.

II. METHODOLOGY

As illustrated in Fig. 1, the proposed approach for damage detection using NARX neural networks in this study involved three stages, (i) sensor clustering, (ii) NARX neural network training, (iii) damage detection.

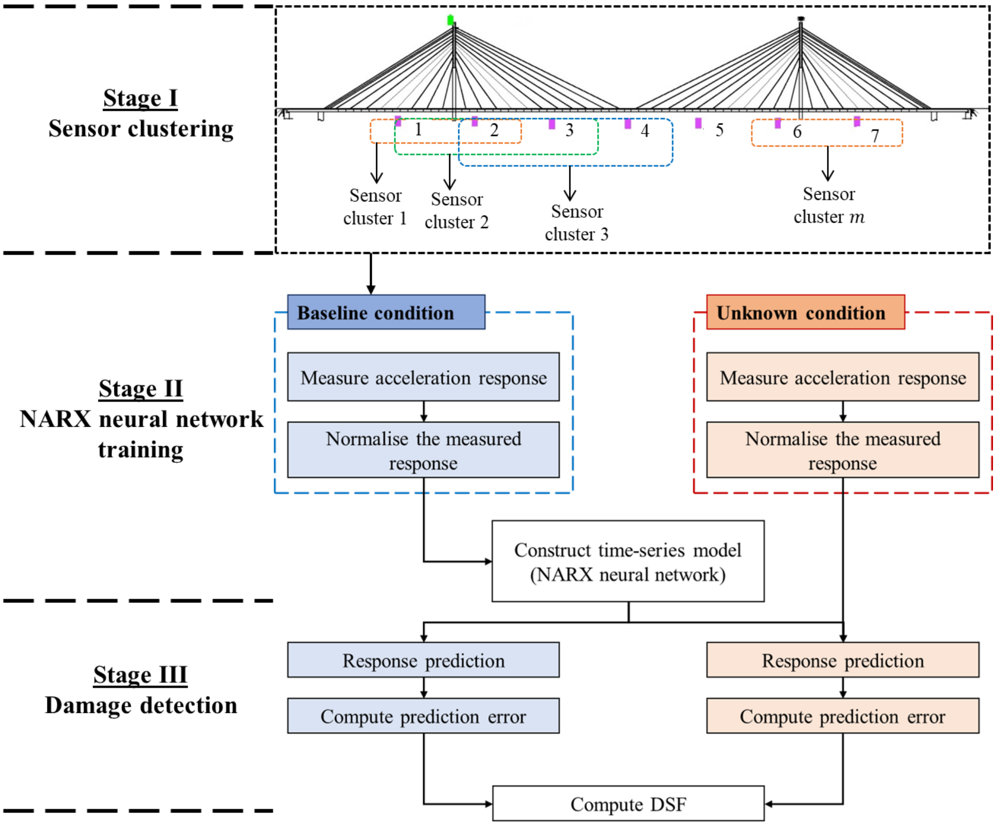

Fig. 1: Damage detection using NARX neural network with sensor clustering

II.I Sensor clustering

Sensor clustering enhances the ability and reduces the complexity of time series approaches for damage detection. In sensor clustering, the structure is addressed as multiple systems rather than a single system. Each system is defined as a cluster where each cluster is monitored by a set of sensors with one assigned as the reference sensor and all the others are classified as neighbour sensors. The acceleration response of the reference sensor will be predicted by the neighbour sensors, which provide input to the NARX neural network. By this means, the reference sensor has two data sets that are predicted from the baseline network and actual measured response. By manipulating these two data sets, DSF can be obtained.

II.II Nonlinear autoregressive with exogenous inputs (NARX) neural network

The concept of neighbour sensors and one reference sensor refers to a multi-input single-output (MISO) system that can be defined through a NARX model. The NARX model is based on the linear ARX model, which is generally used to model a sequence of data points that are observed in time. It made use of the combination of its past output values and those of the input to describe a discrete nonlinear system. The defining equation for the NARX model is:

$$y(t) = f\big(y(t-1), y(t-2), \ldots, y(t-n_y), u(t-1), u(t-2), \ldots, u(t-n_u)\big) \quad (1)$$

in which $y(t)$ denotes the reference sensor response at time step t, f refers to the nonlinear function of the sensor cluster, $u(t)$ is the neighbour sensors response at time step t, and n_y and n_u are the order of output and input, respectively.

ANNs can be used for function approximation, not only for nonlinear systems but also linear systems. Therefore, in this study, the approximation of function f in Equation (1) was implemented in a black-box manner using ANN, henceforth known as NARX neural network.

In this study, series-parallel NARX architecture was adopted since it offers two advantages. The first is that the true output is available during network training and using it as the input to the feedforward network is more accurate. The second is that the resulting network has a purely feedforward architecture and static backpropagation can be used for training. An example schematic representation of the general architecture of a series-parallel NARX neural network for sensor clustering, which is a kind of MISO system, is shown in Fig. 2. It has an input layer with tapped delay lines (TDL), one hidden layer with sigmoid transfer functions and one output layer with a linear transfer function.

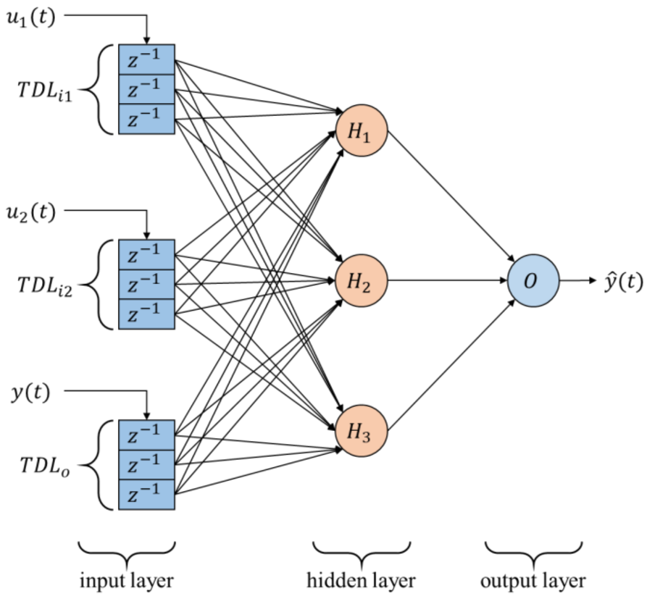

Fig. 2 NARX neural network with two inputs, one output and three hidden neurons

II.III Damage sensitive feature

After time-series models for all sensor clusters under baseline conditions were developed, the same models were used to predict the response under different conditions for the same sensor cluster. The difference between the measured response ($y_m(t)$) and the prediction ($y_p(t)$) was then computed and used to extract DSF. For clarity of notation, let the prediction error of the baseline condition that is known to be undamaged be denoted by $e_U(t)$ and the prediction error of an unknown condition that can be undamaged or damaged be represented by $e_D(t)$. If damage has occurred, the trained networks will no longer give similar prediction performance, where $e_D(t)$ is expected to have larger statistical distributions than $e_U(t)$. As DSF has great consequences on damage detection, three different DSFs correspond to the fit ratio [15], the standard deviation of residual error and the root mean square of residual error, as defined in Equation (2) to (5), are considered in this study. From this point onward, damage features extracted based on standard deviation, fit ratio and root mean square are denoted as $\mathrm{DSF_{SD}}$, $\mathrm{DSF_{FR}}$ and $\mathrm{DSF_{RMS}}$, respectively. The notation $\overline{y_m}$ in Equation (2) is the mean of the measured response and σ in Equation (4) refers to the standard deviation function. Each sensor cluster has its own DSF and by assembling the computed DSF of all clusters, damage can be inferred.

$$FR = 1 - \frac{|y_m - y_p|}{|y_m - \overline{y_m}|} \tag{2}$$

$$DSF_{FR} = \frac{FR_U - FR_D}{FR_U} \tag{3}$$

$$DSF_{SD} = \frac{\sigma(e_D) - \sigma(e_U)}{\sigma(e_U)} \tag{4}$$

$$DSF_{RMS} = \sqrt{\frac{1}{n}\sum_{t=1}^{n} {e_D}^2} - \sqrt{\frac{1}{n}\sum_{t=1}^{n} {e_U}^2} \tag{5}$$

III. NUMERICAL EXAMPLE

To demonstrate the effectiveness of the proposed NARX neural network with sensor clustering approach, numerical model of a two-span concrete slab was used. The slab was modelled using the Structural Dynamics Toolbox in the MATLAB platform. A 4.2 m long, 0.65 m wide and 0.12 m thick slab, as depicted in Fig. 3, was used in this study. The slab was simply supported at 100 mm from each end and the middle span. The presumed material and geometrical properties of the slab were Young's modulus E = 31 GPa, mass density D = 2300 kg/m^3 and Poisson's ratio ρ = 0.2. The finite element modelling of the slab as shown in Fig. 4 was based on four-node quadrilateral shell elements and comprised of a mesh with 105 nodes and 80 elements. The first three frequencies of the simulated slab were 50.95 Hz, 80.51 Hz and 215.8 Hz. A 3% damping ratio was assumed for all modes.

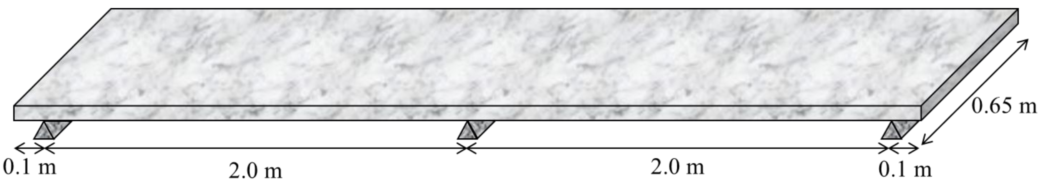

Fig. 3 Two-span slab

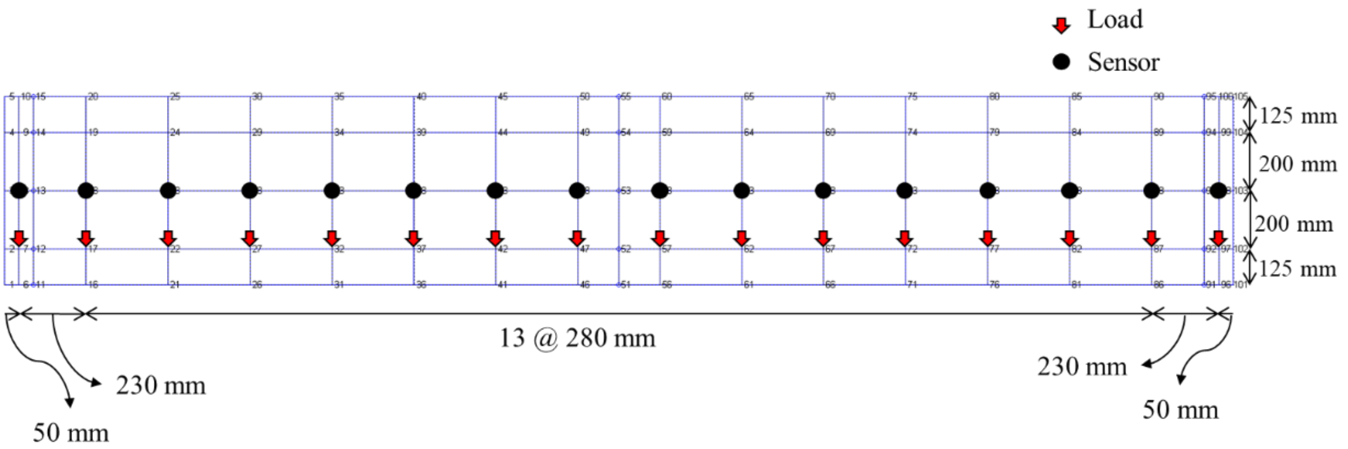

Fig. 4 Finite element model with sensor and load locations

For time response simulation, 16 sensors were assumed to be placed on the centreline of the slab, as given in Fig. 4. To represent ambient excitation, load forces were randomly applied to several points with random magnitude and frequency. The responses of the sensors were computed using Newmark's time integration method. Acceleration data in the vertical direction were recorded by sensors at 500 Hz sampling frequency for a total duration of 110 seconds. However, the first 10 seconds data were ignored to avoid transient effects from start-up [19], whereas the rest of the 100 seconds data were used for damage detection. For damage detection purposes, the slab was divided into 15 equal segments as shown in Fig. 5. Damage was simulated by reducing the *E* value at selected elements and the damage severity was defined in terms of percentage of this reduction.

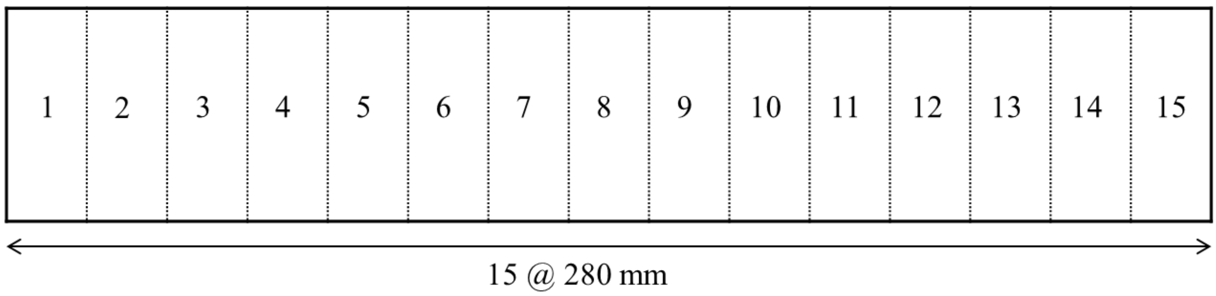

Fig. 5 Considered segments for the slab

III.I Sensor clustering

As described earlier, the concrete slab model with 16 sensors installed along the centreline of the slab was considered. For better representation, these sensors were labelled as in Fig. 6. From this sensor network, 16 different sensor clusters were defined, as given in Table 1. Each cluster was monitored by one reference sensor. Cluster 1 incorporates Sensors 1 and 2, where the first sensor was selected as the reference sensor. Three sensors were included in Clusters 2 through 15, where the reference sensor is the middle one of each cluster. For Cluster 16, Sensors 15 and 16 were incorporated, with the second sensor being the reference sensor.

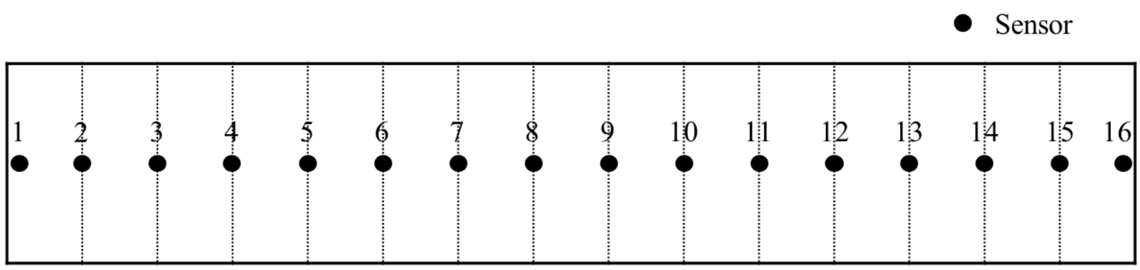

Fig. 6 Sensor numbers for the slab

Table 1: Sensor clustering for a slab with 16 sensors

Cluster	Reference sensor	Neighbour sensor	Cluster	Reference sensor	Neighbour sensor
1	1	2	9	9	8, 10
2	2	1, 3	10	10	9, 11
3	3	2, 4	11	11	10, 12
4	4	3, 5	12	12	11, 13
5	5	4, 6	13	13	12, 14
6	6	5, 7	14	14	13,15
7	7	6, 8	15	15	14, 16
8	8	7, 9	16	16	15

III.II NARX neural network training

After defining all the sensor clusters, NARX neural networks were constructed for each sensor cluster. The 100 s acceleration responses subjected to ambient vibration obtained from the undamaged structure were used in the network training and served as the baseline condition. Before network training, the acceleration response of each sensor was normalised to the [-1 1] range. The normalisation was necessary to not only limit the range of data but also to prevent larger values overriding smaller ones and to avoid the premature saturation of hidden neurons that slows down network training [20]. To apply an early stopping method, the normalised data were randomly partitioned into 70% training, 20% validation and 10% testing sets. The networks were trained using a series-parallel NARX neural network with one hidden layer architecture, the Levenberg-Marquardt algorithm as the learning function, tan-sigmoid as the transfer function in the hidden layer and a linear transfer function in the output layer. In this study, 6^{th} order input and output and 8^{th} order hidden neurons were applied to all sensor cluster networks.

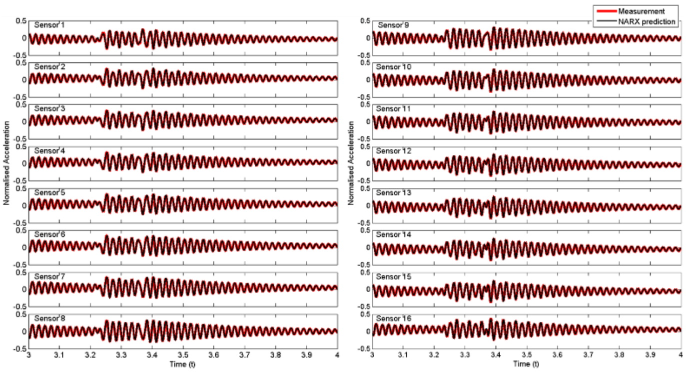

Fig. 7 Sample response of reference sensors and network predictions of the numerical slab at the baseline condition

Fig. 7 shows a 1 s sample of the response estimated using the developed NARX neural networks, which is plotted on top of the acceleration response obtained from the measurement. It is clearly seen that the measured and estimated response match almost perfectly, which indicates that the NARX neural networks fitted the data very well, hence adequately representing the undamaged structural response.

III.III Damage detection

After the NARX neural networks were developed, the acceleration responses from new structural conditions were fed to the network for damage identification response prediction. The concept behind the proposed method in this study is that when damage occurs, the NARX neural network is no longer able to characterise the structural response as the networks are developed based on the undamaged response; hence, the prediction error will be large. By deploying the network prediction error, damage indicators can be extracted and used for damage detection. For implementing the proposed approach, different damage cases, which include single damage as well as multiple damages, were considered. It should be mentioned that the data used in this paper is a noise-free response.

III.III.I Damage at single location

To investigate the sensitivity of the proposed method to damage location, two different damage cases were considered. Each case comprises a single damage site with 30% severity at Segment 4 or 14. Fig. 8 and Fig. 9 depict the obtained DSFs against sensor location for the two damage cases.

Fig. 8 corresponds to the case in which damage is located in the middle of the first span of the slab (Segment 4). Results based on DSF_{SD} (Fig. 8(a)) show that damage is located near Sensors 4 and 5 since the associated DSF at these locations is relatively high compared to other locations. Similar results were also obtained using DSF_{FR} (Fig. 8(b)) and DSF_{RMS} (Fig. 8(c)), which suggest that the three DSFs can provide good indicators for damage presence. Although some false positives appeared at other locations, the highest DSF matched well with the actual simulated damage location. For damage located at Segment 14 (Fig. 9), the detection results showed by the three DSFs follow the same distribution along the slab, where the magnitude is concentrated near Sensor 15 and followed by Sensor 14.

The results presented here demonstrate that the proposed approach based on NARX neural network is sensitive to damage existence. Introducing damage to the slab, resulted in increases in the extracted DSF. The three employed DSFs worked equally well for predicting single damage in the slab. The closer the sensor to the simulated damage location, the higher the predicted value of the corresponding DSF. Therefore, the highest DSF reflects the location of damage.

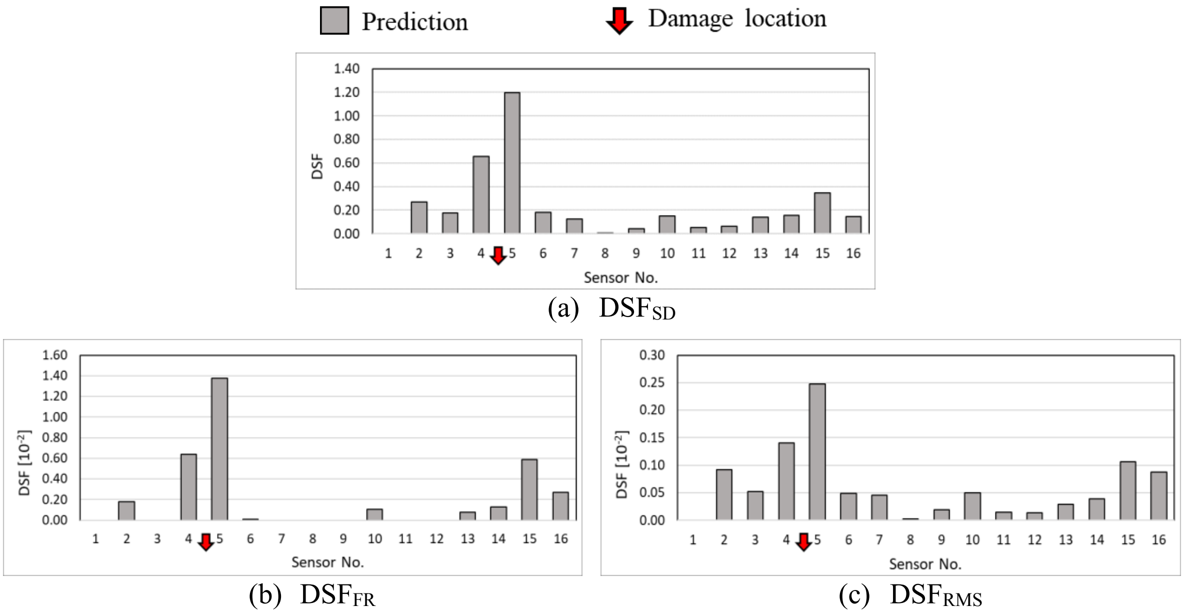

Fig. 8 Prediction of the NARX neural network for damage at Segment 4

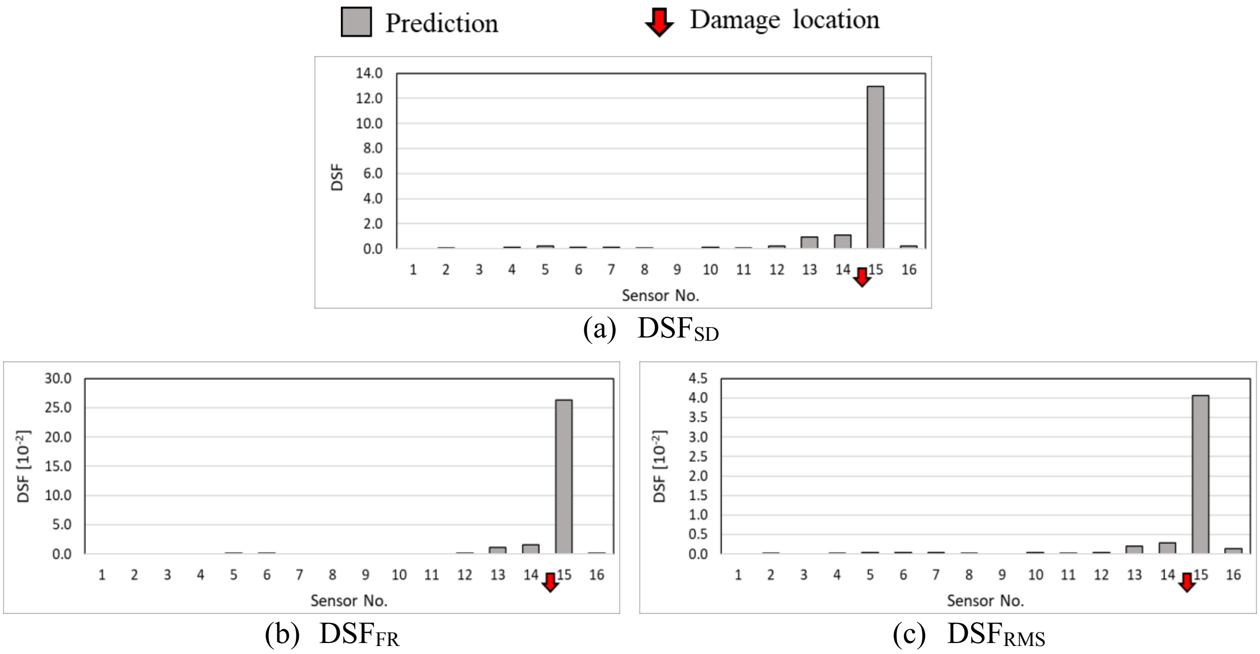

Fig. 9 Prediction of the NARX neural network for damage at Segment 14

III.III.II Effect of damage severity

To investigate the effect of damage severity on the proposed method, the damage case at the first mid-span, as used in the previous section, was considered along with four different damage severities. The reduction of the *E* value at Segment 4 was varied from 10% to 50% in 10% increments. Fig. 10 shows the results obtained using DSF$_{SD}$, DSF$_{FR}$ and DSF$_{RMS}$ for different damage severities. The maximum DSF$_{SD}$ was found near Sensors 4 and 5 for all damage severities, indicating damage was present in that region. Another observation is that the maximum DSF$_{SD}$ increased gradually with the increase of damage severity. The variation of DSF$_{FR}$ and DSF$_{RMS}$ were also in good agreement with damage severity but for a high damage severity (50%), there was a false detection at Sensor 2, where the value was comparable to that predicted at Sensor 4. Nonetheless, the predicted DSF values were still satisfactory to distinguish the damage location. The results in this section are evidence that the developed NARX neural network is good enough in correlating single damage severity with the maximum DSF, hence can be used to relatively quantify the damage severity.

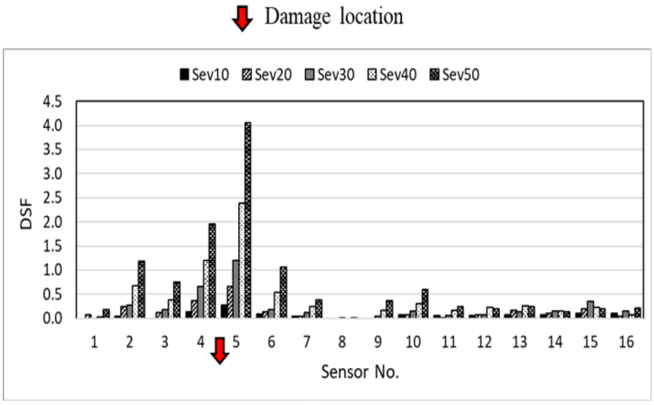

(a) DSF_{SD}

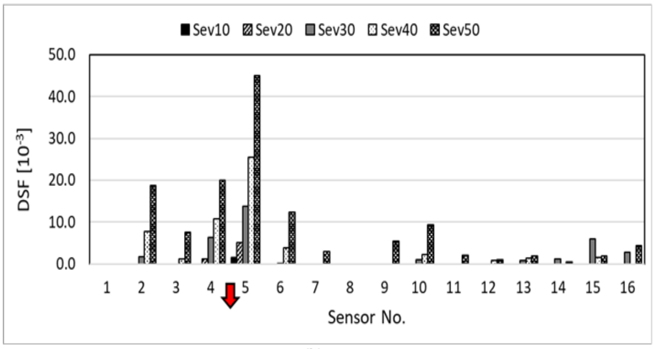

(b) DSF_{FR}

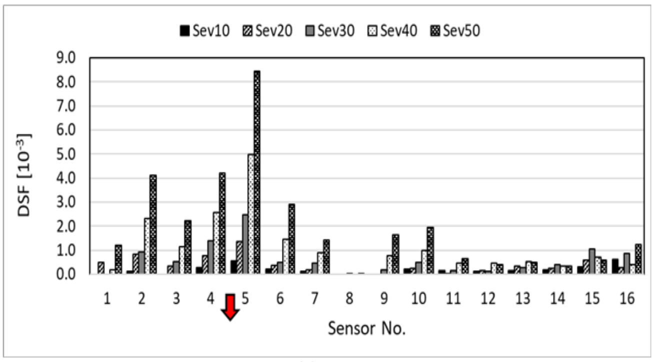

(c) DSF_{RMS}

Fig. 10 Variation of DSF with damage severity

III.III.III Damage at multiple locations

The efficiency of the NARX neural network was further assessed for damage in multiple locations. To achieve this aim, the value of E at Segment 2, 7 and 12 was reduced by 20%, 40% and 30%, respectively. Fig. 11 shows the predicted DSF_{SD}, DSF_{FR} and DSF_{RMS} with sensor location. From the figure, one can observe that each DSF resulted in high values at different locations. In decreasing order of rank, the first three large values identified by DSF_{SD} were at Sensor 13, 2 and 8, while those by DSF_{FR} and DSF_{RMS} were sensor 2, 8 and 13 and 8, 2 and 13, respectively. This observation shows that locations of multiple damage case were successfully detected by the DSFs. However, it has failed to relate the severity of multiple damages with DSF level.

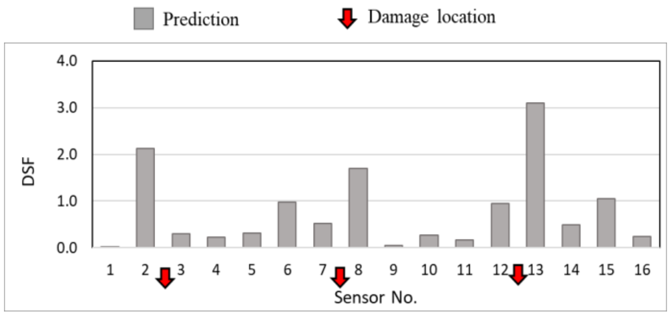

(a) DSF_{SD}

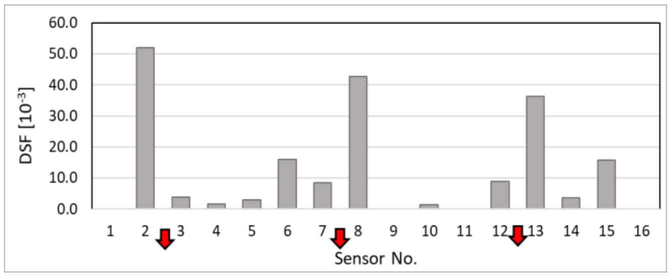

(b) DSF_{FR}

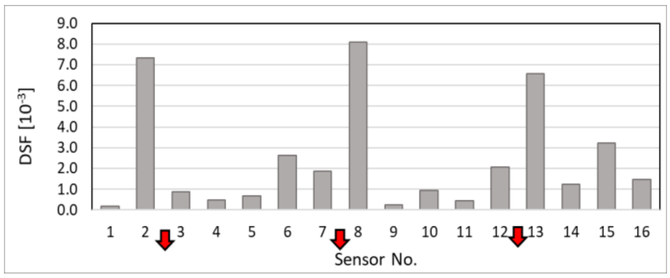

(c) DSF_{RMS}

Fig. 11 Prediction of the NARX neural network for multiple damage case

IV. CONCLUSION

In this paper, a time-series approach for damage detection was presented using noise-free data from numerical model of a two-span concrete slab. The approach is an output-only and non-model damage detection where it solely based on the measured acceleration responses without any need of excitation information or details of physical structural properties. The proposed approach makes use the concept of sensor clustering where the acceleration response of the reference sensor in each cluster at baseline condition is predicted by time-series model. The time series model, namely NARX, was considered and modelled through ANN. If the condition of the structure is no longer the same as the baseline condition, the NARX neural network will result in high prediction error. Based on the prediction error, three DSFs were extracted for damage identification.

The results showed that the proposed time-series approach based on NARX neural networks provides satisfactorily damage detection for single damage and multiple damage cases under ambient vibration. The three employed DSFs were sensitive to damage presence and have approximately the same efficiency in identifying damage. The location of damage can be identified by the highest DSF values. The employed DSFs increase with the severity of single damage. However, in case of multiple damages with different intensities, DSF magnitudes fail to relate to damage severities.

Since the numerical study has proven the applicability of the proposed NARX neural network with sensor clustering approach under noise-free response, future studies should explore the potential of the proposed approach using noisy data since measurement noise is inevitable in real practice. It is also recommended to apply the proposed method using real data obtained from different types of structures and various types of structural damage.

ACKNOWLEDGEMENTS

This study is funded by the Ministry of Higher Education of Malaysia through the LRGS Vot. 4L705 and the HICoE Research Grant Vot. 16J24. The first author gratefully acknowledges the financial support provided by Universiti Teknologi Malaysia and the Ministry of Higher Education, Malaysia.

REFERENCES

[1] Zang, C. and Imregun, M., 2001, "Structural damage detection using artificial neural networks and measured FRF data reduced via principal component projection," J. Sound Vib., 242(5), pp. 813–827.

[2] Kim, M. J., and Eun, H. C., 2017, "Identification of damage-expected members of truss structures using frequency response function," Adv. Mech. Eng., 9(1), pp. 1687814016687911.

[3] Vafaei, M., and Alih, S. C., 2018, "Adequacy of first mode shape differences for damage identification of cantilever structures using neural networks," Neural Comput. Appl., 30(8), pp. 2509–2518.

[4] Wang, S., and Xu, M., 2018, "Modal Strain Energy-based Structural Damage Identification: A Review and Comparative Study," Struct. Eng. Int., 29 (2), pp. 234–248.

[5] Umar, S., Bakhary, N., and Abidin, A. R. Z, 2018, "Response surface methodology for damage detection using frequency and mode shape," Measurement, 115, pp. 258–268.

[6] Fassois, S. D., and Sakellariou, J. S., 2007, "Time-series methods for fault detection and identification in vibrating structures," Philos. Trans. R. Soc. A Math. Phys. Eng. Sci., 365(1851) pp. 411–448.

[7] Roy, K., Bhattacharya, B., and Ray-Chaudhuri, S., 2015, "ARX model-based damage sensitive features for structural damage localization using output-only measurements," J. Sound Vib., 349, pp. 99–122.

[8] Lakshmi, K., Rama Mohan Rao, A., and Gopalakrishnan, N., 2017, "Singular spectrum analysis combined with ARMAX model for structural damage detection," Struct. Control Heal. Monit., 24(9), p. e1960.

[9] Yao, R., and Pakzad, S. N., 2014, "Damage and noise sensitivity evaluation of autoregressive features extracted from structure vibration," Smart Mater. Struct., 23(2) pp. 025007.

[10] Nair, K. K., Kiremidjian, A. S., and Law, K. H., 2006, "Time series-based damage detection and localization algorithm with application to the ASCE benchmark structure," J. Sound Vib., 291(1–2), pp. 349–368.

[11] Sohn, H., and Farrar, C. R., 2001, "Damage diagnosis using time series analysis of vibration signals," Smart Mater. Struct., 10(3), pp. 446–451.

[12] Lu, Y., and Gao, F., 2005, "A novel time-domain auto-regressive model for structural damage diagnosis," J. Sound Vib., 283(3–5), pp. 1031–1049.

[13] Entezami, A., Shariatmada, H. R., and Karamodin, A., 2018, "Data-driven damage diagnosis under environmental and operational variability by novel statistical pattern recognition methods," Struct. Heal. Monit., 18(5–6), pp. 1416–144.

[14] Rytter, A., 1993, "Vibrational Based Inspection of Civil Engineering Structures," PhD Thesis, Dept. of Building Technology and Structural Engineering, Aalborg University.

[15] Gul, M., and Catbas, F. N., 2011, "Structural health monitoring and damage assessment using a novel time series analysis methodology with sensor clustering," J. Sound Vib., 330(6), pp. 1196–1210.

[16] Farahani, R. V., and Penumadu, D., 2016, "Damage identification of a full-scale five-girder bridge using time-series analysis of vibration data," Eng. Struct., 115, pp. 129–139.

[17] Gul, M., and Catbas, F. N., 2011, "Damage Assessment with Ambient Vibration Data Using a Novel Time Series Analysis Methodology," J. Struct. Eng., 137(12), pp. 1518–1526.

[18] Mei, Q., and Gül, M., 2015, "Novel Sensor Clustering–Based Approach for Simultaneous Detection of Stiffness and Mass Changes Using Output-Only Data," J. Struct. Eng., 141(10), p. 04014237.

[19] Yuen, K. V., Au, S. K., and Beck, J. L., 2004, "Two-Stage Structural Health Monitoring Approach for Phase I Benchmark Studies," J. Eng. Mech., 130(1), pp. 16–33.

[20] Basheer, I. A., and Hajmeer, M., 2000, "Artificial neural networks: fundamentals, computing, design, and application," J. Microbiol. Methods, 43(1), pp. 3–31.